Published in final edited form as:
N Engl J Med. 2010 January 21; 362(3): 206–216. doi:10.1056/NEJMoa0900158.

Lethal Skeletal Dysplasia in Mice and Humans Lacking the Golgin GMAP-210

Patrick Smits, Ph.D., **Andrew D. Bolton, B.S.**, **Vincent Funari, Ph.D.**, **Minh Hong, Ph.D.**, **Eric D. Boyden, Ph.D.**, **Lei Lu, Ph.D.**, **Danielle K. Manning, Ph.D.**, **Noelle D. Dwyer, Ph.D.**, **Jennifer L. Moran, Ph.D.**, **Mary Prysak, B.S.**, **Barry Merriman, Ph.D.**, **Stanley F. Nelson, M.D.**, **Luisa Bonafé, M.D., Ph.D.**, **Andrea Superti-Furga, M.D.**, **Shiro Ikegawa, M.D., Ph.D.**, **Deborah Krakow, M.D.**, **Daniel H. Cohn, Ph.D.**, **Tom Kirchhausen, Ph.D.**, **Matthew L. Warman, M.D.**, and **David R. Beier, M.D., Ph.D.**
Orthopedic Research Laboratories, Department of Orthopedic Surgery (P.S., M.H., E.D.B., M.L.W.), the Program in Cellular and Molecular Medicine (L.L., T.K.), and the Howard Hughes Medical Institute (M.L.W.), Children's Hospital; the Division of Genetics, Brigham and Women's Hospital (A.D.B., D.K.M., N.D.D., J.L.M., M.P., D.R.B.); the Immune Disease Institute (L.L., T.K.); and the Departments of Cell Biology (L.L., T.K.) and Genetics (M.L.W.), Harvard Medical School — all in Boston; the Medical Genetics Institute, Cedars–Sinai Medical Center (V.F., D.K., D.H.C.); and the David Geffen School of Medicine, University of California, Los Angeles (V.F., B.M., S.F.N., D.K., D.H.C.) — both in Los Angeles; the Division of Molecular Pediatrics, Centre Hospitalier Universitaire Vaudois, University of Lausanne, Lausanne, Switzerland (L.B.); the Department of Pediatrics, University of Freiburg, Freiburg, Germany (A.S.-F.); and the Center for Genomic Medicine, RIKEN, Tokyo (S.I.)

Abstract

BACKGROUND—Establishing the genetic basis of phenotypes such as skeletal dysplasia in model organisms can provide insights into biologic processes and their role in human disease.

METHODS—We screened mutagenized mice and observed a neonatal lethal skeletal dysplasia with an autosomal recessive pattern of inheritance. Through genetic mapping and positional cloning, we identified the causative mutation.

RESULTS—Affected mice had a nonsense mutation in the thyroid hormone receptor interactor 11 gene (*Trip11*), which encodes the Golgi microtubule-associated protein 210 (GMAP-210); the affected mice lacked this protein. Golgi architecture was disturbed in multiple tissues, including cartilage. Skeletal development was severely impaired, with chondrocytes showing swelling and stress in the endoplasmic reticulum, abnormal cellular differentiation, and increased cell death. Golgi-mediated glycosylation events were altered in fibroblasts and chondrocytes lacking GMAP-210, and these chondrocytes had intracellular accumulation of perlecan, an extracellular matrix protein, but not of type II collagen or aggrecan, two other extracellular matrix proteins. The similarities between the skeletal and cellular phenotypes in these mice and those in patients with achondrogenesis type 1A, a neonatal lethal form of skeletal dysplasia in humans, suggested that achondrogenesis type 1A may be caused by GMAP-210 deficiency. Sequence analysis revealed loss-of-function mutations in the 10 unrelated patients with achondrogenesis type 1A whom we studied.

Address reprint requests to Dr. Warman at the Orthopedic Research Laboratories, Enders 907.2, Children's Hospital, 320 Longwood Ave., Boston, MA 02115, or at matthew.warman@childrens.harvard.edu.

No potential conflict of interest relevant to this article was reported.

CONCLUSIONS—GMAP-210 is required for the efficient glycosylation and cellular transport of multiple proteins. The identification of a mutation affecting GMAP-210 in mice, and then in humans, as the cause of a lethal skeletal dysplasia underscores the value of screening for abnormal phenotypes in model organisms and identifying the causative mutations.

The presence of the Golgi apparatus in all cell types suggests that it is indispensable. Although cultured cells are able to survive when their well-structured Golgi architecture is transiently disrupted chemically or through RNA interference (RNAi),[1] the requirement for an intact Golgi apparatus during development has not been studied. In this article, we describe mice in which the Golgi architecture is disrupted in multiple tissues by a loss-of-function mutation in the thyroid hormone receptor interactor 11 gene (*Trip11*), which encodes the Golgi microtubule-associated protein 210 (GMAP-210 — also known as TRIP230 and TRIP11). Golgins constitute a family of Golgi-associated proteins that serve either as tethering factors that facilitate vesicle fusion to Golgi compartments or as structural proteins that maintain Golgi architecture.[1,2] We observed that mice lacking GMAP-210 die from a skeletal dysplasia that shares phenotypic features with achondrogenesis type 1A, a lethal, autosomal recessive, skeletal dysplasia in humans.[3] We tested for mutations affecting GMAP-210 in patients with achondrogenesis type 1A.

METHODS

IDENTIFICATION AND CHARACTERIZATION OF GMAP-210–DEFICIENT MICE

We carried out a screen for recessive mutations affecting late embryonic development in mice treated with the *N*-ethyl-*N*-nitrosourea (ENU) mutagen, as previously described.[4] We used whole-genome, single-nucleotide-polymorphism (SNP) analysis[5] to map the locus harboring the etiologic mutation and used a polymerase-chain-reaction assay to amplify and sequence candidate genes in accordance with standard methods.

DNA SEQUENCE ANALYSIS OF *TRIP11*

We sequenced *TRIP11* in patients with achondrogenesis type 1A. We confirmed mutations with the use of DNA obtained from patients' parents; in the event that parental DNA was unavailable, we used subcloning followed by sequence analysis to show that the mutant alleles making up a compound heterozygous mutation were derived from different parental chromosomes.

DNA samples from patients with a diagnosis of achondrogenesis type 1A (Online Mendelian Inheritance in Man number, 200600) were provided by three referral centers that specialize in the clinical, radiologic, and histologic characterization of skeletal dysplasia. Each referral center obtained written informed consent to collect and analyze DNA. The institutional review board at Children's Hospital Boston approved the analysis of DNA samples that would be stripped of identifying information before being transferred from the referral centers.

TRANSPORT ASSAY

We prepared adenovirus expressing a temperature-sensitive vesicular stomatitis viral G protein fused to green fluorescence protein ($VSVG^{ts}$–GFP), as previously described.[6] We studied $VSVG^{ts}$–GFP processing in heterozygous and mutant skin fibroblasts grown in six-well culture plates. The assay was repeated three times on separate days and performed in triplicate each time. (See the Supplementary Appendix, available with the full text of this article at NEJM.org, for details on fibroblast cultures; skeletal preparations; histologic analysis; RNA in situ hybridization; electron microscopy; monitoring of chondrocyte

differentiation, proliferation, and apoptosis; immunofluorescence staining of cultured cells and frozen sections; immunodetection of GMAP-210; and an assay for hedgehog signaling.)

RESULTS

TRIP11 AND THE MUTANT MOUSE PHENOTYPE

After initiating mutagenesis with ENU,[4] we identified mice with a neonatal lethal phenotype that was autosomal recessive. Affected mice had short limbs, small thoracic cages, short snouts, domed skulls, and in some cases, omphalocele (Fig. 1A). Skeletal preparations revealed delayed mineralization of intramembranous and endochondral bone (Fig. 1B). As compared with wild-type mice, newborn mutant mice lacked vertebral-body ossification (Fig. 1B). Alveolar formation in the lungs was also decreased in newborn mutant mice as compared with newborn wild-type mice (Fig. 1 in the Supplementary Appendix).

For the screen, we outcrossed mutagenized C57BL/6J mice with wild-type FVB/N mice[4] and used a panel of 394 single-nucleotide polymorphisms (SNPs) spanning the mouse genome to facilitate genetic mapping.[5] After analysis of 10 mutant mice, we located the causative mutation within a 17-Mb region on chromosome 12, and analysis of additional mice narrowed the candidate interval to 3.7 Mb. We sequenced four genes in this interval before identifying a nonsense mutation (c.5003T→A, p.L1668X) in *Trip11* in the mutant mice. Immunoblotting with an antibody that recognizes an epitope encoded by a region of the complementary DNA that precedes the truncating mutation showed that GMAP-210 was absent in protein extracts from mutant cells (Fig. 1C).

To confirm that the phenotype resulted from a mutation in *Trip11*, mice carrying the nonsense mutation were crossed with mice that were heterozygous for another inactivating *Trip11* allele.[7] Offspring that were compound heterozygotes (i.e., carrying the ENU-induced $Trip11^{L1668X}$ nonsense mutation on one allele and a different *Trip11* inactivating mutation on the other allele) had the same phenotype as offspring that were homozygous for the nonsense mutation (data not shown), proving that the phenotype was the result of a GMAP-210 deficiency. We also performed RNA in situ hybridization to determine which tissues normally express *Trip11* messenger RNA (mRNA) and observed widespread expression (Fig. 1D). Therefore, enhanced or restricted expression of GMAP-210 in the developing skeleton does not explain the prominent skeletal phenotype in the mutant animals.

CELLULAR EFFECTS OF GMAP-210 DEFICIENCY

On embryonic day 13.5, wild-type chondrocytes at the centers of humeri start to undergo hypertrophic differentiation, which is associated with an increase in cell size. The humeri of the mutant mice had hypertrophic chondrocytes that were smaller than those in wild-type mice and had proliferating chondrocytes that were larger than those in wild-type mice (data not shown). These differences became more pronounced by embryonic day 15.5, when mutant chondrocytes in the epiphysis and metaphysis were markedly larger than normal (Fig. 1E). Furthermore, mutant chondrocytes failed to form an organized columnar growth zone and produced less extracellular matrix, as indicated by staining with Alcian blue (Fig. 1E).

RNA in situ hybridization with mRNA probes that are specific for proliferating chrondrocytes (*Col2a1*), chondrocytes that are about to undergo hypertrophic differentiation (*Ppr*), and those that are in the early stage of hypertrophic differentiation (*Col10a1*) revealed a delay in differentiation (Fig. 2, and Fig. 2 in the Supplementary Appendix). Expression of *Col2a1* by embryonic day 13.5 was identical in wild-type and mutant mice, whereas expression of the prehypertrophic marker, *Ppr*, and the hypertrophic marker, *Col10a1*, was

reduced in the mutant mice (Fig. 2A in the Supplementary Appendix). By embryonic day 14.5, the expression levels of *Col10a1* in the humeri of mutant mice was similar to that in wild-type mice, but in the mutant mice, the expression domain had not divided into two growth zones, a finding that is consistent with delayed hypertrophic differentiation (Fig. 2A). Furthermore, on embryonic day 14.5, expression of vascular endothelial growth factor (*Vegf*), a marker of late hypertrophic differentiation, and matrix metalloproteinase 13 (M*mp13*), a marker of terminal differentiation, was absent from the mutant humeri, indicating impaired terminal differentiation (Fig. 2A). Finally, on embryonic day 18.5, expression of hypertrophic-differentiation markers became undetectable in the mutant mice (Fig. 2B in the Supplementary Appendix). Thus, chondrocyte hypertrophic differentiation was delayed in the mutant mice, with worsening at later developmental stages and a complete absence of differentiation by embryonic day 18.5.

Since the mutant humeri failed to increase in size, we performed bromodeoxyuridine incorporation assays to assess chondrocyte proliferation. By embryonic day 15.5, there were no proliferating cells in the center of the epiphysis or in the presumptive columnar zone in the humeri of the mutant mice, in contrast to the findings in the wild-type mice (Fig. 2B). The decreased expression of chondrocyte marker genes in the mutant mice on embryonic day 18.5 (Fig. 2B in the Supplementary Appendix) suggested that the chondrocytes were dying. This was confirmed with the use of the terminal deoxynucleotidyl transferase dUTP biotin nick end labeling (TUNEL) assay on embryonic day 17.5, which showed apoptotic chondrocytes throughout mutant humeri but not in wild-type humeri (Fig. 2C).

ENDOPLASMIC RETICULUM AND GOLGI ORGANIZATION AND PROCESSING IN MUTANT CELLS

Transmission electron microscopy of mutant chondrocytes and osteoblasts revealed swelling of the endoplasmic reticulum (Fig. 3A and 3B). Although GMAP-210 was expressed in other cell types (e.g., fibroblasts, endothelial cells, pericytes, myocytes, hepatocytes, and keratinocytes), these cells had endoplasmic reticulum of normal appearance (Fig. 3A in the Supplementary Appendix). Because mutant chondrocytes contained swollen endoplasmic reticulum, we assayed the expression of the endoplasmic reticulum stress-response gene, heat-shock protein 5 (*Hspa5-Bip*),[8] and found that there was greater *Hspa5-Bip* expression in mutant chondrocytes than in wild-type chondrocytes (Fig. 3A in the Supplementary Appendix). Chondrocytes from mutant mice also lacked a typical Golgi apparatus (Fig. 3C). Instead of displaying a Golgi apparatus with stacked cisternal organization, mutant chondrocytes contained an aggregation of vesicle-like structures. Electron microscopical examination of other tissues on embryonic day 15.5 revealed an abnormal Golgi apparatus in the kidney but not in the intestine or lung (Fig. 3C, and Fig. 3C in the Supplementary Appendix). Primary dermal fibroblast cultures from the mutant mice showed an abnormally condensed Golgi apparatus as compared with that in wild-type fibroblasts (Fig. 4A). However, the *cis*- and *trans*-Golgi compartments in the mutant fibroblasts were preserved, as indicated by the adjacent, nonoverlapping localization of Golgi matrix protein 130 (GM130) (a *cis*-Golgi protein) and ADP-ribosylation factor–like 1 (Arl1) (a *trans*-Golgi protein) (Fig. 4A).

Primary chondrocyte cultures from mice lacking GMAP-210 grew poorly and failed to differentiate. Therefore, we used primary skin fibroblasts from mice that were heterozygous or homozygous for the nonsense mutation to evaluate endoplasmic reticulum and Golgi function. We infected these fibroblasts with adenovirus expressing a thermoreversible folding mutant of $VSVG^{ts}$–GFP; this particular mutant is unfolded and retained within the endoplasmic reticulum at 40°C, but it can fold properly and transit through the Golgi apparatus at 32°C (Fig. 4, and Fig. 4A in the Supplementary Appendix). $VSVG^{ts}$–GFP processing differed between homozygous and heterozygous cells (Fig. 4C), probably

because of altered glycosylation of VSVG^{ts}–GFP within the Golgi of homozygous mutant cells rather than impaired transit through the Golgi. We could make this distinction because the transport of VSVG^{ts}–GFP to the cell surface was similar in homozygous and heterozygous cells (Fig. 4 in the Supplementary Appendix).

To confirm that post-translational modifications were altered in cells deficient in GMAP-210, we stained cultured fibroblasts and skeletal sections from wild-type and mutant mice with lectin GS-II. This form of lectin, isolated from the seeds of the tropical African legume *Griffonia simplicifolia*, preferentially binds to the terminal glycan structure *N*-acetylglucosamine.[9] Increased lectin GS-II binding indicates impaired glycosylation because *N*-acetylglucosamine is uncommon in correctly glycosylated proteins. As compared with wild-type fibroblasts, mutant primary dermal fibroblasts showed increased lectin GS-II binding along cell surfaces (Fig. 5 in the Supplementary Appendix), which is consistent with incomplete modification of cell-surface proteins. Furthermore, we observed a marked increase in lectin GS-II binding in the cartilage of mutant mice (as compared with that of wild-type mice), with most of the binding occurring intracellularly (Fig. 5 in the Supplementary Appendix). Lectin GS-II has previously been shown to bind glycans that are being synthesized in the *medial*- and *trans*-Golgi compartments.[10] Therefore, our result is consistent with impaired Golgi function in chondrocytes that lack GMAP-210.

Transmission electron microscopy of the extracellular matrix of cartilage from the humeri revealed that the collagen fibrils were similar in content in wild-type and mutant mice (Fig. 4D). Immunofluorescence light microscopy performed with the use of anti–type II collagen antibodies showed that the amount and distribution of this collagen in the cartilage did not differ between wild-type and mutant mice (Fig. 6 in the Supplementary Appendix), a finding that is consistent with electron-microscopical findings. Similarly, there were no differences between wild-type and mutant mice with respect to antibodies directed against the polypeptide cores of cartilage oligomeric matrix protein and aggrecan (Fig. 6 in the Supplementary Appendix). In contrast, proteoglycan aggregates in cartilage, seen on electron microscopy as granulelike structures, were clearly smaller in the mutant mice than in the wild-type mice (Fig. 4D). Immunofluorescence studies with the use of an antibody directed against the polypeptide core of perlecan showed that mutant chondrocytes had an abnormal accumulation of this protein intracellularly (Fig. 4E), where it partially colocalized with the endoplasmic reticulum marker calreticulin. Perlecan, which is a prominent component of basement membranes, is also secreted by dermal fibroblasts, and fibroblasts from mutant mice retained perlecan intracellularly (Fig. 4F). Therefore, in addition to a general impairment in glycosylation, chondrocytes deficient in GMAP-210 also differ from wild-type chondrocytes in the synthesis and secretion of specific proteins.

MUTATIONS IN *TRIP11* AND ACHONDROGENESIS TYPE 1A

Achondrogenesis type 1A, the neonatal lethal skeletal dysplasia with an autosomal recessive pattern of inheritance seen in our patients (Fig. 5A), has features that are similar to those of the mice with the *Trip11* mutation. The absence of vertebral-body and skull ossification on radiography, the lack of organized columnar zones of proliferating chondrocytes on histologic analysis, the reduced expression of *Col10a1* on immunohistochemical analysis, and the expanded endoplasmic reticulum cisternae in chondrocytes on electron microscopy have all been reported in affected patients.[3,11] We performed sequence analysis of *TRIP11* in our 10 unrelated patients with achondrogenesis type 1A and found loss-of-function mutations in each patient (Fig. 5B). Five mutations create termination codons, four alter the open-reading-frame, and two affect splice sites. Homozygous mutations were present in patients from consanguineous unions, and some mutations were found in more than one family.

DISCUSSION

In 1898, Camillo Golgi described the diffuse reticular network that bears his name.[12] A half-century later, the ribbonlike cisternal architecture of this intracellular structure was observed with an electron microscope.[13] How the Golgi apparatus forms, how it maintains its architecture, and what the relationship is between its structure and its functions — which include glycosylation of proteins — remain incompletely understood.[14] Golgin proteins participate in these processes; ex vivo knockdown of the golgins GMAP-210, golgin-84, and GM130 result in fragmentation of the Golgi apparatus.[15-17] Golgi fragmentation does not completely block the transport and processing of nascent proteins in cultured cells, but it does reduce the efficiency of these processes.[15,16] The identification of mice with a loss-of-function mutation in the gene encoding GMAP-210 facilitates assessment of the function of the Golgi structure in vivo. Although additional roles of GMAP-210 have been suggested,[7,18-20] our in vivo data are most consistent with its role in Golgi organization and protein processing.

Despite expression of GMAP-210 in many cell types, GMAP-210 deficiency altered Golgi architecture and caused swelling of the endoplasmic reticulum in a subgroup of tissues. Cells within the developing skeletal system — chondrocytes and osteoblasts — have very high rates of matrix secretion[21] and may be particularly susceptible to stress when Golgi processing is inefficient. Indeed, chondrocytes with mutant GMAP-210 showed clear evidence of stress in the endoplasmic reticulum, abnormal differentiation, and increased cell death. Impaired protein processing and swelling of the endoplasmic reticulum have been observed in other human skeletal dysplasias. Typically, these dysplasias have been caused by mutations in a secreted matrix protein that impair its folding and secretion. Examples include specific mutations of type I collagen in osteogenesis imperfecta,[22] type II collagen in spondyloepiphyseal dysplasia congenita,[23] type X collagen in Schmid metaphyseal dysplasia,[24] and cartilage oligomeric matrix protein in pseudoachondroplasia and multiple epiphyseal dysplasia.[25] Investigators have identified mutations in patients with craniolenticular dysplasia that affect secretory mutant protein 23A (SEC23A), a protein involved in generating vesicles containing coat protein complex II that are used to move proteins from the endoplasmic reticulum to the Golgi apparatus.[26] The nonlethality of SEC23A deficiency may be explained by the coexpression of its paralog, SEC23B, in most cell types.[27,28] Mutations affecting trafficking protein particle complex 2 (TRAPPC2) and dymeclin, two other proteins thought to have roles in the transport of proteins between the endoplasmic reticulum and the Golgi apparatus, also cause nonlethal skeletal dysplasias — X-linked spondyloepiphyseal dysplasia tarda and the Dyggve–Melchior–Clausen syndrome, respectively.[29-31] Therefore, it is reasonable to postulate that the developing skeleton, being sensitive to defects in protein transport, will be affected by mutations in other components of the secretory pathways whose deficiency causes Golgi disorganization.

Important post-translational modifications, such as the synthesis of glycosaminoglycans, occur in the Golgi apparatus. Chondrocytes produce several highly modified proteoglycans, the most abundant of which is aggrecan, a very large proteoglycan (measuring 500 nm and having a mass of 3 megadaltons) that contains hundreds of glycosaminoglycan side chains.[32] Immunofluorescence studies showed that aggrecan core protein was present in both wild-type and mutant cartilage, even though staining with Alcian blue, electron microscopy, and lectin staining suggest that this protein is improperly glycosylated in the mutant cartilage. In contrast, perlecan, a less abundant and smaller glycosaminoglycan containing proteoglycan, is abnormally retained within mutant chondrocytes and fibroblasts. These data suggest that GMAP-210 maintains the Golgi structure in chondrocytes, thereby facilitating complex glycosylation reactions while also participating in the transport of specific proteins. Indeed, RNAi knockdown of golgin-97 and golgin-245 has been shown to

affect the secretion of E-cadherin and tumor necrosis factor α, respectively. However, depletion of these golgins did not affect the organization of the Golgi apparatus.[33,34]

Loss-of-function mutations in solute carrier family 26, member 2 (*SLC26A2*), which encodes a high-affinity sulfate transporter, cause achondrogenesis type 1B, which is phenotypically similar to achondrogenesis type 1A.[35] Impaired post-translational modification of proteoglycans in cartilage appears to be common to the two disorders.

Follit and colleagues described neonatal lethality in mice with a gene-trap insertion into *Trip11*.[7] Their studies focused on the role of GMAP-210 in the formation of the primary cilia and in intraflagellar transport; they noted that cells from the mutant mice had shorter cilial than those from wild-type mice and that these cells failed to localize intraflagellar transport protein 20 to the Golgi apparatus. Impaired cilial function has previously been shown to cause skeletal-patterning defects as well as skeletal dysplasia through disruption of hedgehog signaling.[36,37] Our data suggest that neither impaired cilial function nor impaired hedgehog signaling is a primary contributor to the skeletal phenotype in mice lacking GMAP-210 (Fig. 7 in the Supplementary Appendix). Decreased alveolar formation was observed in the lungs of gene-trap mutant mice,[7] which we also observed in our mutant mice. We suggest that the lung phenotype is a consequence of the skeletal phenotype, since alveolar deficiency has been observed in other conditions characterized by insufficient thoracic volume.[38]

Although we found *TRIP11* mutations in all 10 patients with achondrogenesis type 1A that were tested, we cannot conclude that every case is attributable to mutations in *TRIP11*. However, the identification of *TRIP11* as the major disease-causing gene makes it possible to conduct genetic testing in families with a history of achondrogenesis type 1A. It is notable that we did not observe missense mutations in patients with achondrogenesis type 1A, suggesting that milder mutations may result in a different clinical phenotype. For example, SNPs near *TRIP11* have been associated with normal variation in human height.[39,40]

Forward genetic analysis has the potential to provide insight into the molecular mechanisms of a biologic process that is novel and unexpected, since a phenotype-driven screen is not biased by preconceptions regarding gene function. In vitro knockdown of GMAP-210 had suggested that the absence of this protein would lead to Golgi fragmentation and dysfunction in all cells. Instead, a forward genetic screen in mutagenized mice indicated that the absence of GMAP-210 predominantly affects the development of the skeletal system. Our finding that patients with achondrogenesis type 1A, a phenotypically similar syndrome, also have mutations in *TRIP11* that lead to GMAP-210 deficiency underscores the power and usefulness of this strategy of genetic inquiry.

Supplementary Material

Refer to Web version on PubMed Central for supplementary material.

Acknowledgments

Supported by grants from the National Institutes of Health (HD36404 and UO1 HD43430, to Dr. Beier; GM075252 and A1063430, to Dr. Kirchhausen; and AR050180, to Dr. Warman) and the Swiss National Research Foundation (320000-116506, to Dr. Bonafe) and by an Arthritis Foundation Investigator Award to Dr. Smits.

We thank the families of patients with achondrogenesis type 1A and their physicians for participating in this study, Drs. W.R. Wilcox and D.L. Rimoin for their clinical expertise, Dr. R. Stottmann for assistance with the hedgehog assay, Dr. G. Pazour for kindly providing the *Trip11* gene-trap mice, and Drs. B. Yoder and Z. Verney for kindly providing the IFT88 mutant mice.

References

1. Barr FA, Short B. Golgins in the structure and dynamics of the Golgi apparatus. Curr Opin Cell Biol. 2003; 15:405–13. [PubMed: 12892780]
2. Sztul E, Lupashin V. Role of tethering factors in secretory membrane traffic. Am J Physiol Cell Physiol. 2006; 290:C11–C26. [PubMed: 16338975]
3. Molz G, Spycher MA. Achondrogenesis type I: light and electron-microscopic studies. Eur J Pediatr. 1980; 134:69–74. [PubMed: 6250850]
4. Herron BJ, Lu W, Rao C, et al. Efficient generation and mapping of recessive developmental mutations using ENU mutagenesis. Nat Genet. 2002; 30:185–9. [PubMed: 11818962]
5. Moran JL, Bolton AD, Tran PV, et al. Utilization of a whole genome SNP panel for efficient genetic mapping in the mouse. Genome Res. 2006; 16:436–40. [PubMed: 16461637]
6. Feng Y, Yu S, Lasell TK, et al. Exo1: a new chemical inhibitor of the exocytic pathway. Proc Natl Acad Sci U S A. 2003; 100:6469–74. [PubMed: 12738886]
7. Follit JA, San Agustin JT, Xu F. The Golgin GMAP210/TRIP11 anchors IFT20 to the Golgi complex. PLoS Genet. 2008; 4(12):e1000315. [PubMed: 19112494]
8. Schröder M, Kaufman RJ. ER stress and the unfolded protein response. Mutat Res. 2005; 569:29–63. [PubMed: 15603751]
9. Puthenveedu MA, Bachert C, Puri S, Lanni F, Linstedt AD. GM130 and GRASP65-dependent lateral cisternal fusion allows uniform Golgi-enzyme distribution. Nat Cell Biol. 2006; 8:238–48. [PubMed: 16489344]
10. Suzaki E, Kataoka K. Lectin cytochemistry in the gastrointestinal tract with special reference to glycosylation in the Golgi apparatus of Brunner's gland cells. J Histochem Cytochem. 1992; 40:379–85. [PubMed: 1552177]
11. Aigner T, Rau T, Niederhagen M, et al. Achondrogenesis Type IA (Houston-Harris): a still-unresolved molecular phenotype. Pediatr Dev Pathol. 2007; 10:328–34. [PubMed: 17638425]
12. Golgi C. Intorno allla struttura delle cellule nervose. Bollettino della Societa Medico-chirurgica di Pavia. 1898; 13:3–16.
13. Dalton AJ, Felix MD. Cytologic and cytochemical characteristics of the Golgi substance of epithelial cells of the epididymis in situ, in homogenates and after isolation. Am J Anat. 1954; 94:171–207. [PubMed: 13148119]
14. Pfeffer SR. Unsolved mysteries in membrane traffic. Annu Rev Biochem. 2007; 76:629–45. [PubMed: 17263661]
15. Diao A, Rahman D, Pappin DJ, Lucocq J, Lowe M. The coiled-coil membrane protein golgin-84 is a novel rab effector required for Golgi ribbon formation. J Cell Biol. 2003; 160:201–12. [PubMed: 12538640]
16. Marra P, Salvatore L, Mironov A Jr, et al. The biogenesis of the Golgi ribbon: the roles of membrane input from the ER and of GM130. Mol Biol Cell. 2007; 18:1595–608. [PubMed: 17314401]
17. Rios RM, Sanchis A, Tassin AM, Fedriani C, Bornens M. GMAP-210 recruits gamma-tubulin complexes to cis-Golgi membranes and is required for Golgi ribbon formation. Cell. 2004; 118:323–35. [PubMed: 15294158]
18. Lee JW, Choi HS, Gyuris J, Brent R, Moore DD. Two classes of proteins dependent on either the presence or absence of thyroid hormone for interaction with the thyroid hormone receptor. Mol Endocrinol. 1995; 9:243–54. [PubMed: 7776974]
19. Chang KH, Chen Y, Chen TT, et al. A thyroid hormone receptor coactivator negatively regulated by the retinoblastoma protein. Proc Natl Acad Sci U S A. 1997; 94:9040–5. [PubMed: 9256431]
20. Beischlag TV, Taylor RT, Rose DW, et al. Recruitment of thyroid hormone receptor/retinoblastoma-interacting protein 230 by the aryl hydrocarbon receptor nuclear translocator is required for the transcriptional response to both dioxin and hypoxia. J Biol Chem. 2004; 279:54620–8. [PubMed: 15485806]
21. Aszódi A, Bateman JF, Gustafsson E, Boot-Handford R, Fassler R. Mammalian skeletogenesis and extracellular matrix: what can we learn from knockout mice? Cell Struct Funct. 2000; 25:73–84. [PubMed: 10885577]

22. Lisse TS, Thiele F, Fuchs H, et al. ER stress-mediated apoptosis in a new mouse model of osteogenesis imperfecta. PLoS Genet. 2008; 4(2):e7. [PubMed: 18248096]
23. Seegmiller RE, Bomsta BD, Bridgewater LC, et al. The heterozygous disproportionate micromelia (dmm) mouse: morphological changes in fetal cartilage precede postnatal dwarfism and compared with lethal homozygotes can explain the mild phenotype. J Histochem Cytochem. 2008; 56:1003–11. [PubMed: 18678883]
24. Tsang KY, Chan D, Cheslett D, et al. Surviving endoplasmic reticulum stress is coupled to altered chondrocyte differentiation and function. PLoS Biol. 2007; 5(3):e44. [PubMed: 17298185]
25. Piróg-Garcia KA, Meadows RS, Knowles L, et al. Reduced cell proliferation and increased apoptosis are significant pathological mechanisms in a murine model of mild pseudoachondroplasia resulting from a mutation in the C-terminal domain of COMP. Hum Mol Genet. 2007; 16:2072–88. [PubMed: 17588960]
26. Boyadjiev SA, Fromme JC, Ben J, et al. Cranio-lenticulo-sutural dysplasia is caused by a SEC23A mutation leading to abnormal endoplasmic-reticulum-to-Golgi trafficking. Nat Genet. 2006; 38:1192–7. [PubMed: 16980979]
27. Lang MR, Lapierre LA, Frotscher M, Goldenring JR, Knapik EW. Secretory COPII coat component Sec23a is essential for craniofacial chondrocyte maturation. Nat Genet. 2006; 38:1198–203. [PubMed: 16980978]
28. Fromme JC, Ravazzola M, Hamamoto S, et al. The genetic basis of a craniofacial disease provides insight into COPII coat assembly. Dev Cell. 2007; 13:623–34. [PubMed: 17981132]
29. Gedeon AK, Tiller GE, Le Merrer M, et al. The molecular basis of X-linked spondyloepiphyseal dysplasia tarda. Am J Hum Genet. 2001; 68:1386–97. [PubMed: 11349230]
30. Dimitrov A, Paupe V, Gueudry C, et al. The gene responsible for Dyggve-Melchior-Clausen syndrome encodes a novel peripheral membrane protein dynamically associated with the Golgi apparatus. Hum Mol Genet. 2009; 18:440–53. [PubMed: 18996921]
31. Osipovich AB, Jennings JL, Lin Q, Link AJ, Ruley HE. Dyggve-Melchior-Clausen syndrome: chondrodysplasia resulting from defects in intracellular vesicle traffic. Proc Natl Acad Sci U S A. 2008; 105:16171–6. [PubMed: 18852472]
32. Heinegård D, Wieslander J, Sheehan J, Paulsson M, Sommarin Y. Separation and characterization of two populations of aggregating proteoglycans from cartilage. Biochem J. 1985; 225:95–106. [PubMed: 3977833]
33. Lock JG, Hammond LA, Houghton F, Gleeson PA, Stow JL. E-cadherin transport from the trans-Golgi network in tubulovesicular carriers is selectively regulated by golgin-97. Traffic. 2005; 6:1142–56. [PubMed: 16262725]
34. Lieu ZZ, Lock JG, Hammond LA, La Gruta NL, Stow JL, Gleeson PA. A trans-Golgi network golgin is required for the regulated secretion of TNF in activated macrophages in vivo. Proc Natl Acad Sci U S A. 2008; 105:3351–6. [PubMed: 18308930]
35. Superti-Furga A, Hästbacka J, Wilcox WR, et al. Achondrogenesis type IB is caused by mutations in the diastrophic dysplasia sulphate transporter gene. Nat Genet. 1996; 12:100–2. [PubMed: 8528239]
36. Haycraft CJ, Serra R. Cilia involvement in patterning and maintenance of the skeleton. Curr Top Dev Biol. 2008; 85:303–32. [PubMed: 19147010]
37. Wong SY, Reiter JF. The primary cilium at the crossroads of mammalian hedgehog signaling. Curr Top Dev Biol. 2008; 85:225–60. [PubMed: 19147008]
38. American Thoracic Society. Mechanisms and limits of induced postnatal lung growth. Am J Respir Crit Care Med. 2004; 170:319–43. [PubMed: 15280177]
39. Lettre G, Jackson AU, Gieger C, et al. Identification of ten loci associated with height highlights new biological pathways in human growth. Nat Genet. 2008; 40:584–91. [PubMed: 18391950]
40. Gudbjartsson DF, Walters GB, Thorleifsson G, et al. Many sequence variants affecting diversity of adult human height. Nat Genet. 2008; 40:609–15. [PubMed: 18391951]

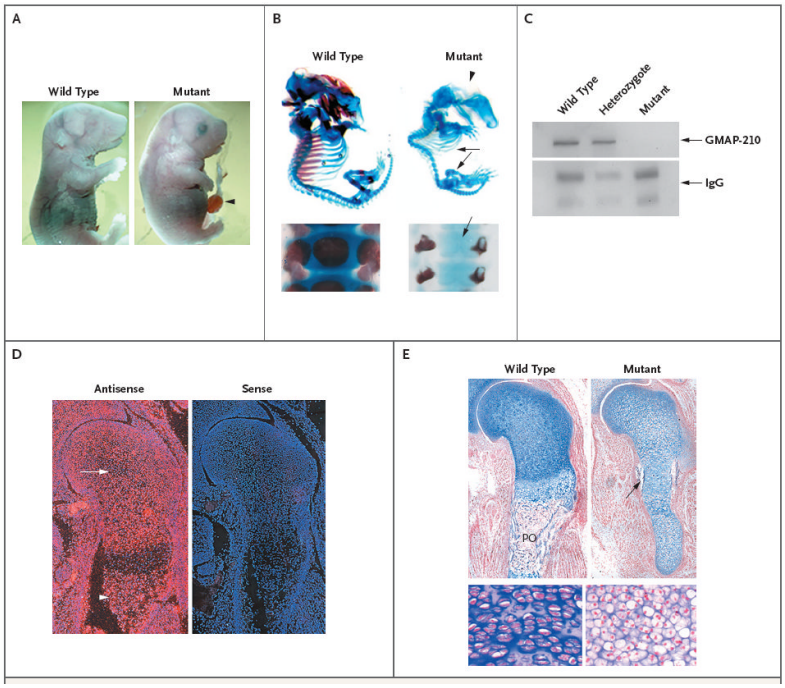

Figure 1. Effects of *Trip11* Mutation in Mice

Panel A shows a wild-type fetal mouse and a fetal mouse with an induced nonsense mutation in *Trip11*, the gene encoding GMAP-210, on embryonic day 18.5. The mouse with the mutation has a domed skull, short snout, short trunk, short limbs, and omphalocele (arrowhead). In Panel B (top), the staining of cartilage with Alcian blue and bone with alizarin red on embryonic day 17.5 in a wild-type mouse and a mouse with the *Trip11* mutation reveals the absence of mineralization in the skull (arrowhead), rib cage, and limbs (arrows) in the mutant. In Panel B, bottom, staining of cartilage and bone in the vertebral columns of newborn wild-type and mutant mice reveals the absence of mineralization in the vertebral body of the mutant (arrow). In Panel C, immunoblotting of GMAP-210 in immunoprecipitated samples of primary skin fibroblasts from a wild-type mouse, a heterozygous mouse, and a mutant mouse shows that GMAP-210 is not detectable in the mutant fibroblasts. IgG, which was used in the immunoprecipitation reaction, also serves as a loading control. In Panel D, in situ hybridization of specimens of wild-type shoulder girdle and humerus obtained on embryonic day 15.5, with the use of *Trip11* antisense and sense RNA probes, shows the expression of *Trip11* in all cell types, with an absence of increased expression in cartilage (arrow) and bone (arrowhead). Red indicates *Trip11* mRNA expression. The nuclei of cells have been stained with 4′,6-diamidino-2-phenylindole, which fluoresces blue. Panel E shows histologic sections of the shoulder girdle and humerus from wild-type and mutant mice, obtained on embryonic day 15.5 and stained with nuclear-fast red and Alcian blue. The cartilage in the mutant humerus shows less staining with Alcian blue and contains chondrocytes with increased cell sizes. The mutant specimen also lacks an organized growth zone of flattened chondrocytes and a primary ossification (PO) center, although it does have a bone collar (arrow). Higher magnification images from the wild-type and mutant growth zones show the increased size of chondrocytes and the lack of chondrocyte columnar organization in the mutant cartilage.

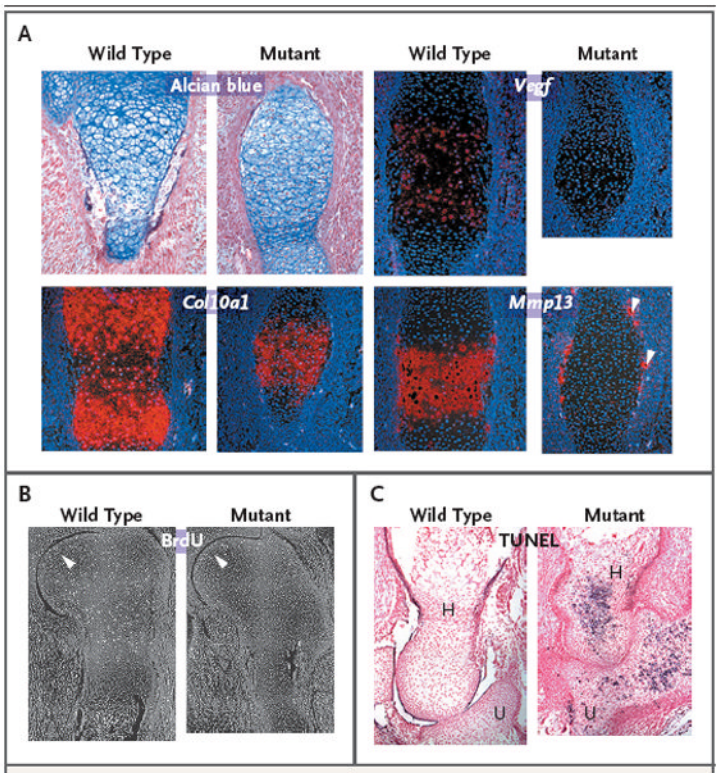

Figure 2. Effects of GMAP-210 Deficiency on Hypertrophic Differentiation, Proliferation, and Apoptosis of Chondrocytes in Mice

Panel A shows sections through the primary ossification centers of humeri from wild-type and mutant mice that were obtained on embryonic day 14.5, stained with Alcian blue, and subjected to in situ hybridization. *Col10a1* expression has not separated into two domains in the mutant humerus, and there is no cartilage expression of the late-stage hypertrophic chondrocyte markers vascular endothelial growth factor (*Vegf*) and matrix metalloproteinase 13 (*Mmp13*). *Mmp13* is expressed only by periosteal osteoclasts in the mutant humerus (arrowheads). Sections through shoulder joints and humeri obtained on embryonic day 15.5 show that there is no difference in the incorporation of bromodeoxyuridine (BrdU) between wild-type and mutant chondrocytes adjacent to the joint (Panel B, arrowheads) but that in the mutant cartilage there is no other area of BrdU incorporation. Use of the terminal deoxynucleotidyl transferase dUTP biotin nick end labeling (TUNEL) assay on histologic sections of elbow joints obtained on embryonic day 17.5 show that the mutant humerus (H) and ulna (U) have many TUNEL-positive cells, which appear blue in the sections, whereas the wild-type humerus and ulna do not (Panel C).

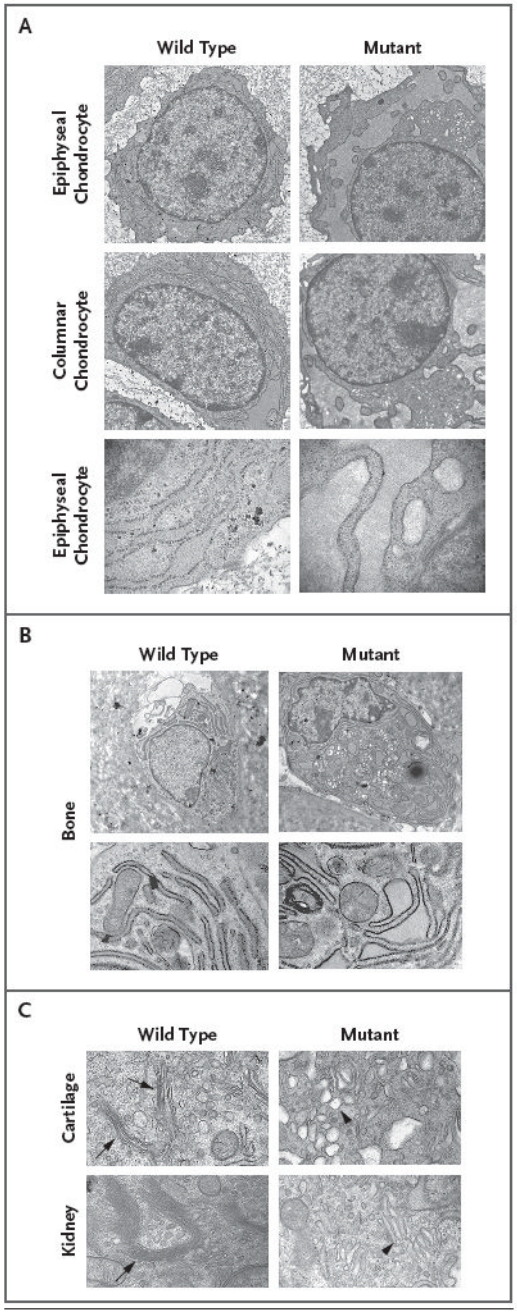

Figure 3. Swollen Endoplasmic Reticulum Cisternae and Abnormal Golgi Architecture in Murine Chondrocytes Lacking GMAP-210

Electron micrographs of chondrocytes from wild-type and mutant humeri obtained on embryonic day 15.5 show increased swelling of the endoplasmic reticulum in epiphyseal and columnar chondrocytes in mice lacking GMAP-210 (Panel A), as compared with their wild-type counterparts. A higher-magnification view of the epiphyseal chondrocytes showing ribosomes along the membrane surface of swollen cisternae in the mutant indicates that this is part of the endoplasmic reticulum. Electron micrographs of osteoblasts from the bone collar of wild-type and mutant humeri (Panel B, top row, and at higher magnification in the bottom row) show increased swelling of the endoplasmic reticulum in the mutant osteoblast. Panel C shows Golgi stacks in wild-type cartilage cells obtained on embryonic day 13.5 (top

row, arrows) and wild-type kidney cells obtained on embryonic day 15.5 (bottom row, arrow) but not in mutant cells. The Golgi apparatus in the mutant cells consists of a collection of vesicles and enlarged cisternae (arrowheads).

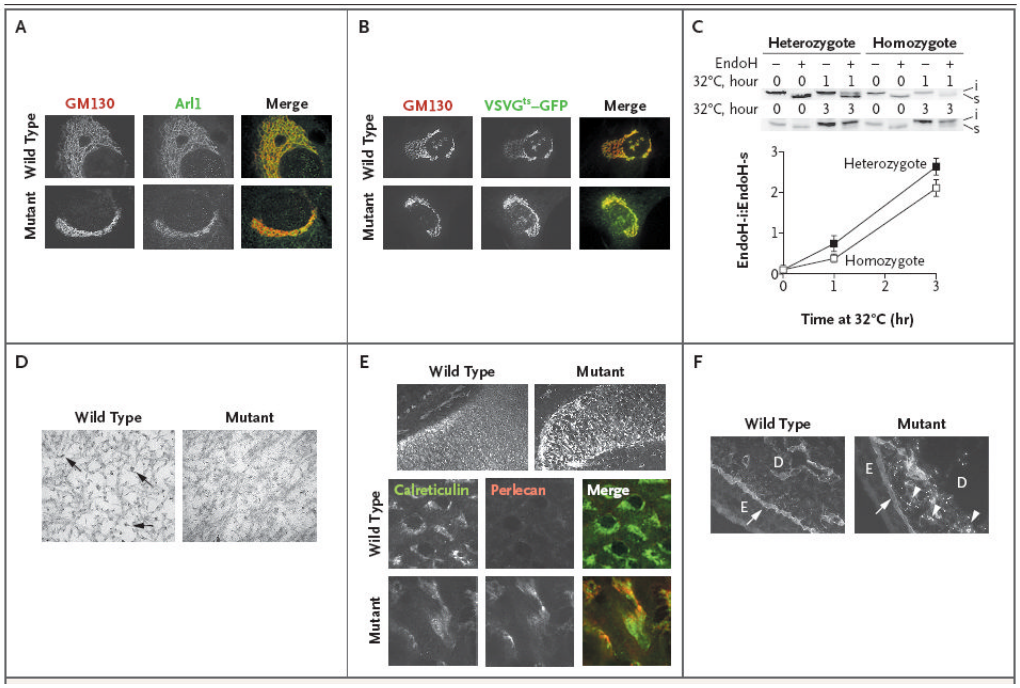

Figure 4. Impaired Post-Translational Protein Processing and Secretion in Murine Cells Lacking GMAP-210

Panel A shows immunofluorescence staining for GM130, a *cis*-Golgi protein, and Arl1, a *trans*-Golgi protein, in wild-type and mutant primary skin fibroblasts. The immunofluorescence staining shows that mutant fibroblasts lack the reticular pattern that is present in wild-type fibroblasts and instead have small vesicles that contain these Golgi-associated proteins. The gray scale is used to indicate fluorescence in the images for which only one protein is shown, and color is used for the merged images in which both proteins are shown. The merged images show that the structures containing GM130 (red) and Arl1 (green) do not overlap in wild-type or in mutant fibroblasts. Although the appearance of the Golgi apparatus differs between mutant fibroblasts and wild-type fibroblasts, the lack of overlap between GM130-containing vesicles and Arl1-containing vesicles indicates that mutant fibroblasts maintain the *cis-trans* polarity of the Golgi apparatus. Panels B and C show the results of a transport assay performed with vesicular stomatitis viral G protein fused to green fluorescence protein (VSVG^{ts}–GFP) in wild-type and mutant primary skin fibroblasts. In Panel B, fluorescence localization of VSVG^{ts}–GFP and immunofluorescence localization of GM130 was performed in wild-type and mutant primary skin fibroblasts after the temperature of the infected cells had been shifted from 40°C to 32°C for 20 minutes. The gray scale is used to indicate fluorescence in the images for which only one protein is shown, and color is used for the merged images in which both proteins are shown. The merged images show that VSVG^{ts}–GFP (green) and GM130 (red) have substantial overlap (yellow) in wild-type and in mutant cells, indicating that transport from the endoplasmic reticulum to the Golgi apparatus is not blocked in mutant cells. Panel C shows a Western blot analysis of a representative VSVG^{ts}–GFP transport assay and a graph depicting the means (±SD) of three independent experiments using primary skin fibroblasts from mice that were heterozygous or homozygous for the *Trip11* mutation. After 1 hour and 3 hours at 32°C, cells that were completely lacking GMAP-210 (homozygous) had a lower mean ratio of endoglycosidase H–insensitive (endoH-i) VSVG^{ts}–GFP to endoglycosidase H–sensitive (EndoH-s) VSVG^{ts}–GFP than heterozygous cells; this finding is consistent with the view that the efficiency of Golgi glycosylation is reduced in fibroblasts with mutant GMAP-210.

In Panel D, electron micrographs of extracellular matrix from epiphyseal cartilage in wild-type and mutant humeri, obtained on embryonic day 17.5, show that the density of collagen fibrils is similar but that the glycosaminoglycan-containing complexes, which normally collapse and appear granular after the electron-microscopical fixation process (arrows), are smaller in the mutant extracellular matrix. Panel E shows changes in the distribution of perlecan (which can be seen with immunofluorescence detection and are depicted in the gray scale) between histologic sections of wild-type and mutant humeri obtained on embryonic day 15.5 (top row). At higher magnification, immunofluorescence detection of perlecan (red) and the endoplasmic reticulum protein calreticulin (green) shows that mutant chondrocytes have greater retention of perlecan within their endoplasmic reticulum than do wild-type chondrocytes, as indicated by the stronger intracellular fluorescence and partial overlap (yellow) with calreticulin in the merged image. In Panel F, immunofluorescence detection of perlecan in the skin of wild-type and mutant mice on embryonic day 15.5 shows an accumulation of perlecan in the mutant dermal fibroblasts (arrowheads). The arrows indicate the epidermal basement membrane; E denotes epidermis, and D dermis.

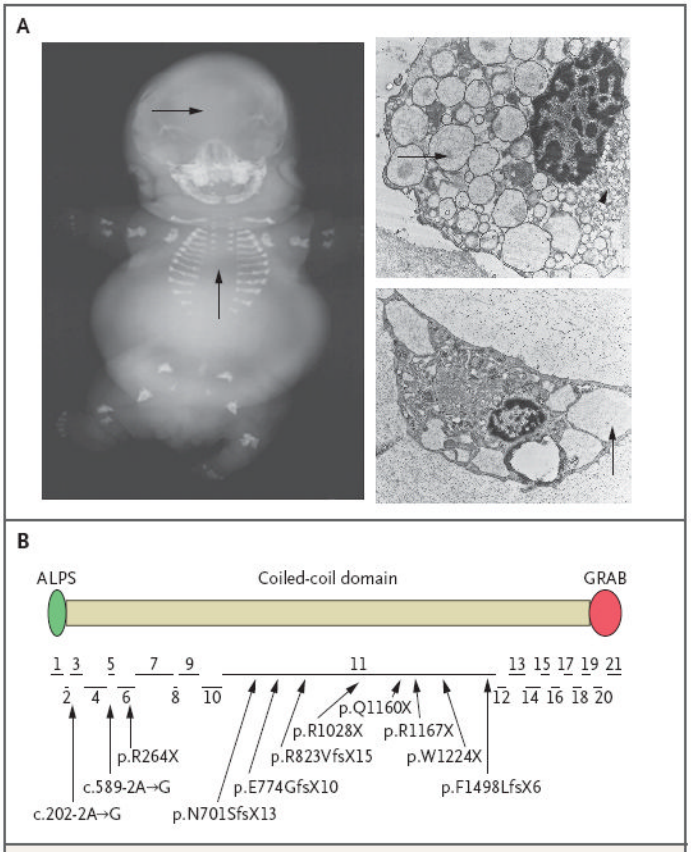

Figure 5. Mutations in *TRIP11* and Human Achondrogenesis Type 1A

In Panel A, a radiograph of a 27-week-old human fetus with a diagnosis of achondrogenesis type 1A reveals a lack of mineralization in the skull and the vertebral column (arrows) and short limbs. The electron micrographs at the right show chondrocytes from two unrelated fetuses with achondrogenesis type 1A, with swollen endoplasmic reticulum (arrows) and vesicular Golgi apparatus (arrowhead in upper image). In Panel B, the structure of the GMAP-210 protein is shown with the relative location and sizes of its 21 coding exons indicated below. ALPS (amphipathic lipid sensor domain) and GRAB (GRIP-related Arf-binding domain) reportedly mediate interactions between GMAP-210 and membranes in vitro. In the diagram below the protein, arrows point from the mutations that were identified in 10 unrelated patients with achondrogenesis type 1A to their approximate locations within the exons. Two mutations (c.202-2A→G and c.589-2A→G) affect intronic splice-acceptor sites. Five mutations (p.R264X, p.R1028X, p.Q1160X, p.R1167X, and p.W1224X) are nonsense mutations. The remaining mutations are frameshift mutations. Several patients, including those from consanguineous unions, were homozygous for mutations, whereas others were compound heterozygotes. Some mutations were found in more than one patient.